AD A095014

WSRL-0171-TM

AR-002-036

DEPARTMENT OF DEFENCE

DEFENCE SCIENCE AND TECHNOLOGY ORGANISATION

WEAPONS SYSTEMS RESEARCH LABORATORY

DEFENCE RESEARCH CENTRE SALISBURY
SOUTH AUSTRALIA

TECHNICAL MEMORANDUM

WSRL-0171-TM

LOW-SPEED WIND-TUNNEL TESTS OF TWO WEATHERCOCKING SENSORS

D.P. BROWN and R.I. MACLEOD

THE UNITED STATES NATIONAL TECHNICAL INFORMATION SERVICE IS AUTHORISED TO REPRODUCE AND SELL THIS REPORT

DTIC FILE COPY

DTIC SELECTE FEB 1 3 1981 A

Approved for Public Release

COPY No. 25

© Commonwealth of Aust

AUGUST 1980

(9) Technical memorandum

AR-002-036

DEPARTMENT OF DEFENCE

DEFENCE SCIENCE AND TECHNOLOGY ORGANISATION

WEAPONS SYSTEMS RESEARCH LABORATORY

(11) July X

(12) 33

TECHNICAL MEMORANDUM

(14) WSRL-0171-TM

(6) # LOW-SPEED WIND-TUNNEL TESTS OF TWO WEATHERCOCKING SENSORS

(10) D.P. Brown and R.I. Macleod

SUMMARY

Two blunt-nosed weathercocking wind direction sensors, one stabilised by a ring tail and the other by swept cruciform fins, were tested in a low-speed wind tunnel to investigate possible aerodynamic interference between these wind direction sensors and the vehicles in front of which they were to be mounted. In these low speed tests, sensor support shaft diameter and vehicle nose tip geometry both caused significant errors in the ring-tailed sensor's alignment to the free stream when the vehicle was at angle of attack. A disk baffle placed on the shaft behind the sensor base was found to reduce sensor misalignment significantly at small angles of attack. Alignment errors for the cruciform sensor were much smaller than those of the ring-tailed sensor at small angles of attack, and these smaller errors were further reduced when a baffle was placed on the shaft.

...n For
...ed
...ion

A

POSTAL ADDRESS: Chief Superintendent, Weapons Systems Research Laboratory, Box 2151, GPO, Adelaide, South Australia, 5001.

DOCUMENT CONTROL DATA SHEET

Security classification of this page: UNCLASSIFIED

1 DOCUMENT NUMBERS	2 SECURITY CLASSIFICATION
AR Number: AR-002-036	a. Complete Document: Unclassified
Report Number: WSRL-0171-TM	b. Title in Isolation: Unclassified
Other Numbers:	c. Summary in Isolation: Unclassified

3 TITLE

LOW-SPEED WIND-TUNNEL TESTS OF TWO WEATHERCOCKING SENSORS

4 PERSONAL AUTHOR(S):

D.P. Brown and R.I. Macleod

5 DOCUMENT DATE:

August 1980

6 6.1 TOTAL NUMBER OF PAGES: 25

6.2 NUMBER OF REFERENCES: 4

7 7.1 CORPORATE AUTHOR(S):

Weapons Systems Research Laboratory

7.2 DOCUMENT SERIES AND NUMBER

Weapons Systems Research Laboratory 0171-TM

8 REFERENCE NUMBERS

a. Task: DST 77/027

b. Sponsoring Agency:

9 COST CODE:

10 IMPRINT (Publishing organisation)

Defence Research Centre Salisbury

11 COMPUTER PROGRAM(S) (Title(s) and language(s))

12 RELEASE LIMITATIONS (of the document):

Approved for Public Release

12.0	OVERSEAS	NO		P.R.	1	A		B		C		D		E	

Security classification of this page: UNCLASSIFIED

Security classification of this page: UNCLASSIFIED

13 ANNOUNCEMENT LIMITATIONS (of the information on these pages):

No limitation

14 DESCRIPTORS:

a. EJC Thesaurus Terms

Wind tunnel tests
Detectors
Wind direction
Accuracy
Alignment
Weathercocking sensors
Velocity pursuit guidance
Base flows
Vortices
Aerodynamic interference
Stability
Light homing

b. Non-Thesaurus Terms

15 COSATI CODES:

1707
2004

16 LIBRARY LOCATION CODES (for libraries listed in the distribution):

17 SUMMARY OR ABSTRACT:
(if this is security classified, the announcement of this report will be similarly classified)

Two blunt-nosed weathercocking wind direction sensors, one stabilised by a ring tail and the other by swept cruciform fins, were tested in a low-speed wind tunnel to investigate possible aerodynamic interference between these wind direction sensors and the vehicles in front of which they were to be mounted. In these low speed tests, sensor support shaft diameter and vehicle nose tip geometry both caused significant errors in the ring-tailed sensor's alignment to the free stream when the vehicle was at angle of attack. A disk baffle placed on the shaft behind the sensor base was found to reduce sensor misalignment significantly at small angles of attack. Alignment errors for the cruciform sensor were much smaller than those of the ring-tailed sensor at small angles of attack, and these smaller errors were further reduced when a baffle was placed on the shaft.

TABLE OF CONTENTS

LIST OF FIGURES

1. INTRODUCTION

Under DST Task 77/027 "Terminally Guided Weapons (Aerodynamics and Performance)", Aeroballistics Division has been investigating means of implementing velocity pursuit guidance of unpowered vehicles using semi-active laser seekers. To implement velocity pursuit guidance it is necessary to measure the angle between the missile's velocity vector and the line of sight to the target. An effective means of doing this is to mount the target seeker ahead of the missile nose so that is is free to weathercock into the free stream. The aim of this study is to determine how accurately such devices will align themselves parallel to the undisturbed free stream.

This Memorandum only reports on preliminary low-speed wind-tunnel tests of two such sensors. More accurate high-speed tunnel tests are currently being performed and will be reported by M.L. Robinson of Aerodynamics Research Group in due course.

The devices tested are blunt-nosed to accommodate the lens (or radome) of a laser (or other) seeker, are free to rotate about a two-axis universal joint centred at the centre of gravity of the weathercocking portion of the device, have blunt open bases to permit sensor rotations of up to 20^0, and are fin stabilised. The two sensors considered are shown in figures 1 and 2. The Mk I and II sensors are stabilised by a ring tail and cruciform fins respectively. The ring tail offers advantages of robustness and smaller wing span but suffers from higher aerodynamic drag. The Mk I sensor was designed to be mounted in front of a rocket-boosted unpowered "Dart"(ref.1) where there was sufficient scope in vehicle design to ensure adequate venting of the air flowing through the ring tail. The Mk II sensor, however was designed to sit in front of a Mk 82 bomb(ref.2) with the constraint that the sensor be fully retracted during aircraft carriage so that the bomb would remain short enough to be compatible with the BRU-3 rack. If a ring tail were used in this case it would have to surround the bomb's conical nose (semi-angle 14^0) posing a considerable design problem at transonic speeds if drag during aircraft carriage is to be minimised. The sensors will be described in more detail in Section 2.

The test method and results obtained will be discussed in Sections 3 and 4 respectively. Three vehicle nose shapes and four shaft diameters were tested with the Mk I sensor, while a single nose shape and shaft diameter were tested with the Mk II sensor.

At the low speed of these tests, 49 m/s, the Reynolds number based on sensor body diameter is approximately 0.15 million. At this relatively low Reynolds number some instability in the laminar flow over the sensor body was observed, which led to undamped oscillations of the sensor, particularly the Mk II sensor which had a much freer pivot than the Mk I sensor. Both smoke filaments and cotton tufts were used to visualise the flow.

Because the sensors were placed just ahead of relatively large vehicles their alignments were influenced by upwash produced by vehicle angle of attack. For the Mk I sensor, however, the misalignment for vehicle angle of attack less than about five degrees was much larger than could be explained in terms of upwash. Flow visualisations suggested that the toroidal vortex behind the sensor body becomes grossly distorted when the shaft and/or nose tip are displaced from their symmetrical, zero-incidence positions. The flow field distortion evidently is such that it has much greater influence on the ring tail than on the cruciform tail.

In an attempt to limit the strength of the toroidal vortex (and also to displace it downstream) a 25 mm diameter circular disk (baffle) was placed on the shaft at various distances behind the sensors. When placed about 0.75

sensor body diameters behind the sensor it was quite successful in greatly reducing the low-incidence misalignments suffered by the Mk I (ring tailed) sensor. Whether this is purely a low Reynolds number phenomenon could not be resolved in the low speed tunnel; proposed tests in the high speed (S1) tunnel may do so, as well as revealing Mach number effects

2. MODELS

The configurations tested are shown in figures 1 and 2. Both sensor bodies consist of an ellipsoidal nose, with a tip radius of curvature of 16 mm, which is faired to a cylindrical afterbody.

The ring tail dimensions were chosen to give the Mk I sensor an estimated static margin of at least 5 mm throughout the Mach number range 0 to 4, the minimum occurring near Mach 1. Below Mach 0.8 and above Mach 1.2 the static margin should exceed 14 mm, or 20% of body length. For the Mk II sensor a static margin of at least 23 mm, or 32% of body length, was estimated for subsonic and transonic speeds; it was not thought that this sensor would be used at higher speeds.

In practice, a substantial static margin is desirable to provide sufficient torque at low sensor angles of attack to overcome asymmetric torques due to electrical leads passing from sensor to missile, sensor lateral mass offset, pivot stiction, and so on. At the same time the aft location of large fins produces the pitch damping moments required to damp out sensor oscillations induced mainly by wind gusts.

The universal joint (pivot) of the Mk I sensor was essentially a pair of yokes pinned to an 8 mm cube of PTFE. This joint deteriorated somewhat during the tests, having to be replaced once, so, for the Mk II sensor joint, the PTFE and pins were replaced by a metal cross and four 12 mm ball races.

Various shaft diameters and missile nose shapes were investigated with the Mk I sensor; the variations are shown in figure 1. The mildly convex nose shape designated nose A was designed to have the maximum volume compatible with unobstructed airflow through the ring tail when the shaft and sensor are fully retracted - assuming that in some applications it may be desirable to have the sensor retracted before and during missile launch. The noses B and C were chosen to show the effects of concavity and increased convexity respectively. The chosen shaft diameters range from so thin that stiffness could be a problem, to so thick that sensor rotation is restricted. The thickest shaft is of a similar proportion to that used on the Texas Instruments' PAVEWAY II laser guided bomb.

Since the wind tunnel test section is 300 mm square, the "missile" supporting the sensor was limited to 75 mm diameter and 150 mm length. Because the Mk I and Mk II sensors were being tested at full scale and a third scale respectively, only a small portion of the front ends of the Dart(ref.1) and Mk 82 bomb respectively could be modelled.

Both models were constructed so that the shaft length could be varied. This was regarded as an important parameter because for various structural reasons it is desirable to have the shortest acceptable shaft length.

"Baffles" on the shaft were tested with both configurations. Their geometry is shown in figures 1 and 2. For the Mk 1 sensor, the baffle was only used with the 8 mm shaft. The baffle diameter was chosen so that the baffle would be inside the separated flow region behind the sensor body until the missile angle of attack exceeded about 10^{0}.

3. TEST METHOD

The Aeroballistics Division low-speed tunnel has a 300 mm square test section and operates at atmospheric pressure and speeds up to 49 m/s, giving a maximum Reynolds number of 0.15 million based on a sensor body diameter of 46 mm. The model was supported from a circular section in one side wall of the tunnel. Angle of attack of the supporting model was varied by rotating this section. To read sensor angle of attack, a hair line was visually aligned parallel to the base of the Mk I sensor ring tail, or to lines painted on the Mk II sensor fins, and the angle between this hair line and the tunnel axis was measured with a protractor. A repeatability of about 0.2^0 was generally obtained by this method (figure 3).

The tests comprised setting the supporting model at a sequence of angles of attack within the range $\pm 15^0$ and measuring the corresponding sensor angles of attack. This procedure was repeated for various combinations of supporting body nose shape, shaft diameter (Mk I sensor only), baffle on or off, and sensor-body separation distance ("X" in figures 1 and 2), as indicated in Table 1.

In the series of tests listed in the top row of Table 1, cotton tufts were attached to the sensor, shaft and supporting-body nose in an attempt to define the flowfield. This provided useful information as will be discussed in a later section. Some crude smoke visualisation was also attempted and again was useful, although the tunnel speed had to be reduced to 5 m/s to ensure stable smoke filaments, reducing the Reynolds number based on sensor diameter to a rather low 15 000. For these tests, the aerodynamic forces were too weak to overcome stiction in the pivot, so the sensor attitude had to be set at angles appropriate to the supporting model angle of attack as determined by previous tests at maximum tunnel speed.

4. DISCUSSION OF RESULTS

4.1 Mk I sensor

Alignment of the Mk I sensor to the free stream direction is given in figure 4 for noses A, B and C. The shaft diameter in each case was 8 mm. Since ideally the sensor angle of attack (α_s) is an odd symmetrical function of missile angle of attack (α_m), average values of α_s, have been plotted versus α_m. The sensor alignment was virtually independent of nose shape when the separation distance (X) was greater than about 135 mm (ie about 3 sensor body diameters). For separations less than about 90 mm (or 2 diameters) the alignment, for α_m less than one degree, was highly perturbed; for example, with nose A and X = 90 mm, α_s changed from $+1.4^0$ to -1.4^0 as α_m changed from -0.2^0 to $+0.2^0$, while with nose C the sensor oscillated violently when α_m was less than 0.5^0 for all X less than 90 mm.

Since the rate of change of α_s with α_m near $\alpha_m = 0$ is an important parameter, it is presented in figure 5 as a function of X for noses A, B and C with a shaft diameter of 8 mm in each case. For X between 100 and 135 mm, nose C is best with respect to this parameter, but rapidly becomes worst at smaller X. For nose A, $(\partial\alpha_s/\partial\alpha_m)_{\alpha=0}$ exhibits a resonance-like

peak centred on X = 85 mm, while nose B exhibits a slight peaking at a similar value of X. This amplification is presumably related to the fact that when X is about 85 mm, the cavity between the sensor base and the missile nose is roughly the same size as the toroidal vortex which forms behind the sensor when X is large.

Cotton tufts on the missile nose showed that when the flow separating at the sensor base reattaches on the missile nose, small missile angles of attack induce what appear to be large cross flow velocities on the missile nose. It is suggested that this contributes to asymmetrical development of the toroidal vortex. Moreover, the wake behind the sensor flows exclusively down the leeward surface of the missile for missile angles of attack as small as 1 or 2^0. These asymmetries induce upwash at the stabilising ring tail. The flowfield for small angle of attack, as deduced from the quite crude flow visualisation tests, is sketched in figure 6.

From such a model, one can predict (qualitatively) that increasing missile nose cross-sectional area or surface slope at the reattachment line, or equivalently, increasing shaft diameter when X is large, should increase $(\partial a_s/\partial a_m)_{a=0}$. The steady deterioration with nose B for decreasing X is due to the fact that both nose cross-sectional area and surface slope at the reattachment line are increasing as X decreases. For decreasing X, the convex nose A eventually almost fills the cavity behind the sensor so that no large-scale vortex can develop; hence the superiority of nose A for X less than 65 mm.

The effect of shaft diameter (d_{sh}) is seen in figure 7. In these tests the shaft length was so long that the misalignments were virtually independent of missile geometry. For α_m (and hence shaft angle of attack) less than about 5^o, the sensor misalignment increases almost in direct proportion to shaft diameter (for d_{sh} up to at least 45% of sensor body diameter). For larger α_m, the downwash at the ring tail (in the angle of attack plane) in the flow immediately ahead of the larger diameter shafts becomes important, cancelling a significant proportion of the upwash induced by both the asymmetrical basal vortex and the missile (plus shaft) angle of attack. The theoretical upwash due to the missile alone was estimated from reference 3 and, as shown in figure 7, is much smaller than that required to produce the observed sensor misalignments.

4.2 Mk I sensor plus baffle

Having postulated that the low angle of attack perturbations in sensor alignment are associated with asymmetry of the toroidal votex behind the sensor, it was further postulated that these perturbations may be reducible by suitably interfering with the development of such vortices. If this were possible the shaft length required to achieve a given relative alignment accuracy might be reduced significantly. Since the more subtle approach of varying the missile nose geometry had only been partially successful, a more brutal approach seemed justified. Consequently it was proposed that a disk should be placed on the shaft in such a position that its circumference lies near the core of the toroidal vortex; the appropriate disk diameter was chosen to be 25 mm (roughly 50% of sensor base diameter). A small toroidal vortex will be generated between the sensor base and the disk, with smaller vortices behind the disk. This vortex pattern should not be as susceptible to resonant-cavity type amplification as was the original configuration.

Baffle (disk) diameter was not varied in the tests conducted, but distance, Y, between sensor and baffle was varied as shown in Table 1(a).

Figure 8 shows the effects of the baffle in various positions for the cases X = 75, 90, 105 and 135 mm for nose B. (Recall that X is distance between sensor and missile). For X up to 105 mm, when the baffle is about 10 mm behind the ring tail base (and hence 32.5 mm behind the sensor base, see figure 1, the sensitivity of α_s to α_m is reduced by a factor of at least 4 for α_m up to 1^o. At angles of attack greater than about 8^o the baffle has an almost insignificant effect. When X equals 135 mm the missile causes only minor interference to the toroidal vortex, so the effect of the baffle is now to reduce interference between the shaft and the vortex; the optimum position of the baffle in this case is nearer the plane of the ring-tail base. If the baffle is placed more than a sensor diameter aft of the sensor base it interacts with the vortex in much the same way as a missile nose in the same position - compare case X = 135, Y = 30 to case X = 90 with no baffle.

The baffle was generally most effective when it was placed about 10 mm aft of the ring tail base, although insufficient tests were completed to fully justify this statement. The maximum reductions in misalignment sensitivity for both noses A and B are given in figure 9. These results confirm rather conclusively that the low angle of attack sensor misalignments are strongly influenced by the nature of the toroidal vortex behind the sensor and, furthermore, that these misalignments can be significantly reduced by modifying the development of that vortex.

Some pertinent work by Mair(ref.4) has recently come to the authors' attention. In that work, Mair studied experimentally the effect of a rear-mounted disc on the drag of a blunt-based body of revolution. For a disc diameter equivalent to 27 mm, base drag reductions of up to 25% were observed, the greatest reduction occurring when the disc was placed a distance equivalent to 37 mm aft of the sensor base (that is, about 14 mm aft of the ring tail base). Although that study was restricted to axisymmetric flows, it seems significant that the disc location that minimises base drag is similar to that which was here found to minimise sensor alignment sensitivity to missile (or shaft) angle of attack.

4.3 Mk II sensor

Testing of the Mk II sensor was much less exhaustive than for the Mk I sensor. The influences of shaft diameter and missile nose shapes upon the flowfield were assumed to be virtually independent of sensor fin configuration, so only the effect of varying baffle position was investigated.

Alignment of the Mk II sensor to the free stream direction is given in figure 10 for the single shaft/nose combination tested. Except for large separation distances, the sensor tilted in the same sense as the missile for angles of attack less than about 3.5^o. This phenomenon is opposite that observed with the Mk I sensor - recall figure 3 - but of rather smaller magnitude. While a plausible interpretation of the flowfield could be offered for the Mk I (ring-tail) case, the interpretation for the Mk II (cruciform) case is less obvious, possibly involving second order features of the flowfield which could not be detected by the methods used in the present tests. For angles of attack greater than 3.5^o, the sensor alignment was consistent with the sense expected to be produced by upwash ahead of the missile, and decreased with increasing separation distance.

For values of X up to 70 mm and for angles of attack less than a critical value (which varied from 10 degrees at X = 25 mm to 1.5^0 at X = 70 mm), the Mk II sensor executed sustained oscillations. These are believed to be due to flow separation on the sensor body at the low Reynolds numbers of the tests. The higher pivot friction and larger shoulder radius of curvature of the Mk I sensor model would both reduce the probability of observing oscillations in the tests of that model.

4.4 Mk II sensor plus baffle

The effect of the baffle is summarised in figure 11. The baffle when at Y = 10 mm had virtually no effect, but when at Y = 20 mm it removed both the positive tilt and the undamped sensor oscillations at low angles of attack. Assuming that the baffle reduced disturbances near the rear of the sensor body sufficiently to reduce or eliminate flow separation on the sensor body, it is possible that higher Reynolds numbers would produce a similar result. Proposed tests in the S1 high speed tunnel may verify this.

5. CONCLUSIONS

These crude low-speed wind-tunnel tests of two wind-direction sensors which are mounted a short distance in front of a missile's nose tip indicate that:

(a) mounting shaft diameter and missile nose tip geometry can have a significant influence on the sensor alignment;

(b) the ringtail sensor suffers the greater misalignments, particularly at low missile angles of attack, and;

(c) a means (such as a baffle on the shaft) of modifying the strength or position of the toroidal vortex behind the sensor may improve sensor performance, although this might well only apply at the rather low Reynolds numbers of the present tests.

6. ACKNOWLEDGEMENTS

The author is grateful to Mr M.L. Robinson and Mr C. Jermey for their advice on aerodynamic design of the wind vanes and planning the tests and to technical staff of Aerodynamics Research Group for assistance in conducting the tests.

NOTATION

X	distance between sensor and supporting body (see figures 1 and 2)
Y	distance between sensor and "baffle" (see figures 1 and 2)
d_b	diameter of sensor body
d_{sh}	shaft diameter
α_m	missile angle of attack
α_s	sensor angle of attack

REFERENCES

No.	Author	Title
1	Brown, D.P.	"A proposed rocket launched vehicle for testing terminal guidance concepts". WRE-TR-1927(W), January 1978 (C)
2	Brown, D.P. and Lloyd, K.H.	"Aerodynamic considerations of a gliding munition based on the Mk 82 bomb". WSRL-0058-TM, November 1978 (R)
3	Letko, W. and Danforth III, E.C.B.	"Theoretical investigation at subsonic speeds of the flow ahead of a slender inclined parabolic-arc body of revolution and correlation with experimental data obtained at low speeds". NACA TN 3205, July 1954
4	Mair, W.A.	"The effect of a rear-mounted disc on the drag of a blunt-based body of revolution". The Aeronautical Quarterly, Vol. 16, November 1965, pp 350-360

TABLE 1. SUMMARY OF TESTS

(a) Mk I Sensor

Nose	Shaft diameter (mm)	Baffle	X (mm)	Y (mm)	Remarks
A	8	No	50,55,60,75,90 105,120,135,155,175	-	(a)
A	8	Yes	75 90 105 135	-10,-5,5 -10,5,15 -10,5,15 -10,-5	(a)
B	8	No	45,60,75,90,105, 120,135,155		
B	8	Yes	60 75 90 105 135	-5 0,5,10 -10,0,5,10 -5,0,5,10 -5,0,5,10,20,30	
C	8	No	30,45,60,75,90, 105,135,155		
C	8	Yes	90	5	
A	5 14 20	No	155		
B	5	No	155		
C	5	No	155		
A A A	14 8 -	No Yes No	155 90 -	- 15 -	(b) (b) (b)(c)

Remarks: (a) With cotton tufts to visualise flow
(b) With smoke to visualise flow; tunnel speed = 5 m/s
(c) Without sensor or shaft

TABLE 1(CONTD.).

(b) Mk II Sensor

Baffle	X (mm)	Y (mm)
No	25,40,55,70,100,150	
Yes	42 55 70	20 10,20,30 20

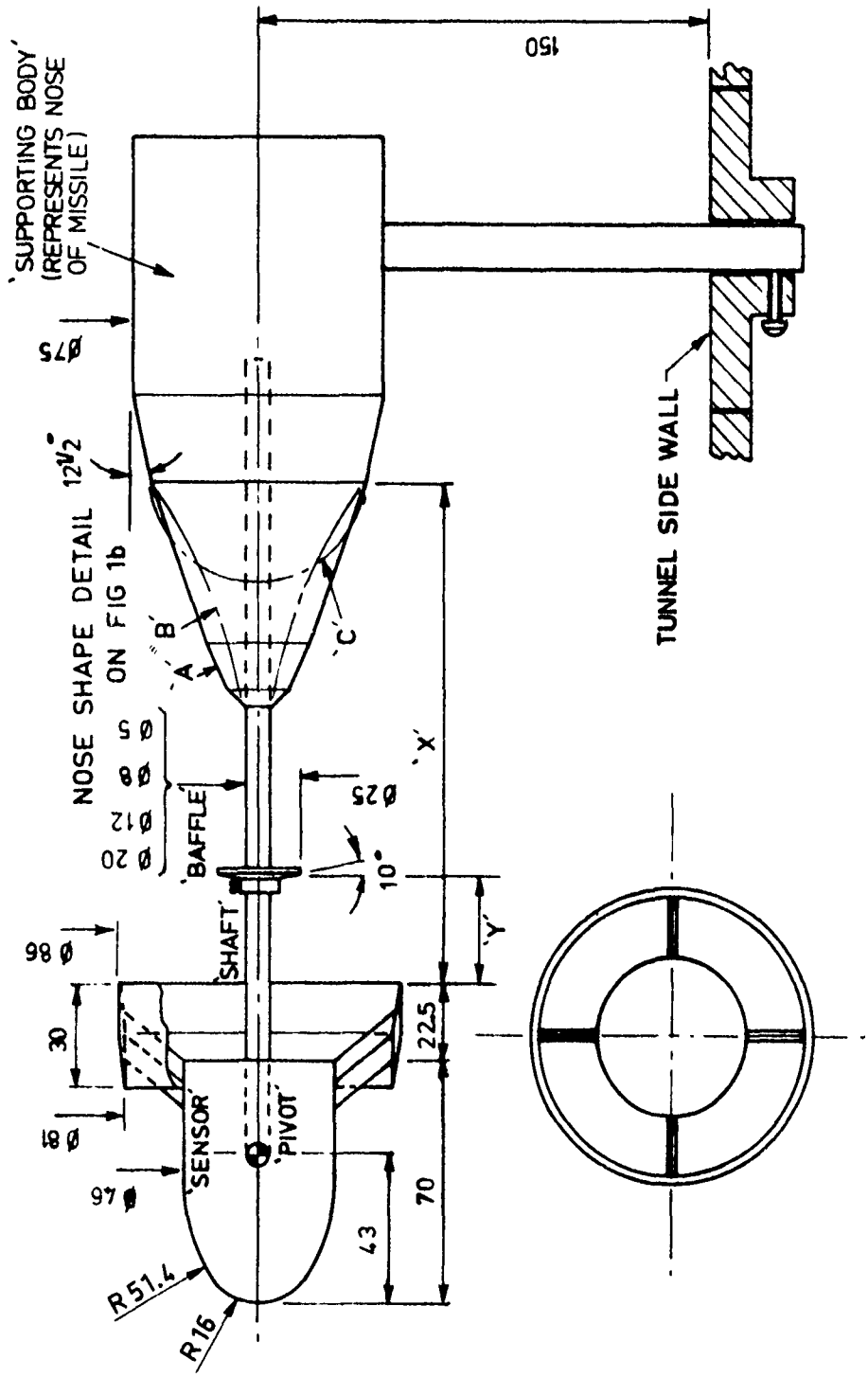

Figure 1(a). Mk1 wind direction sensor

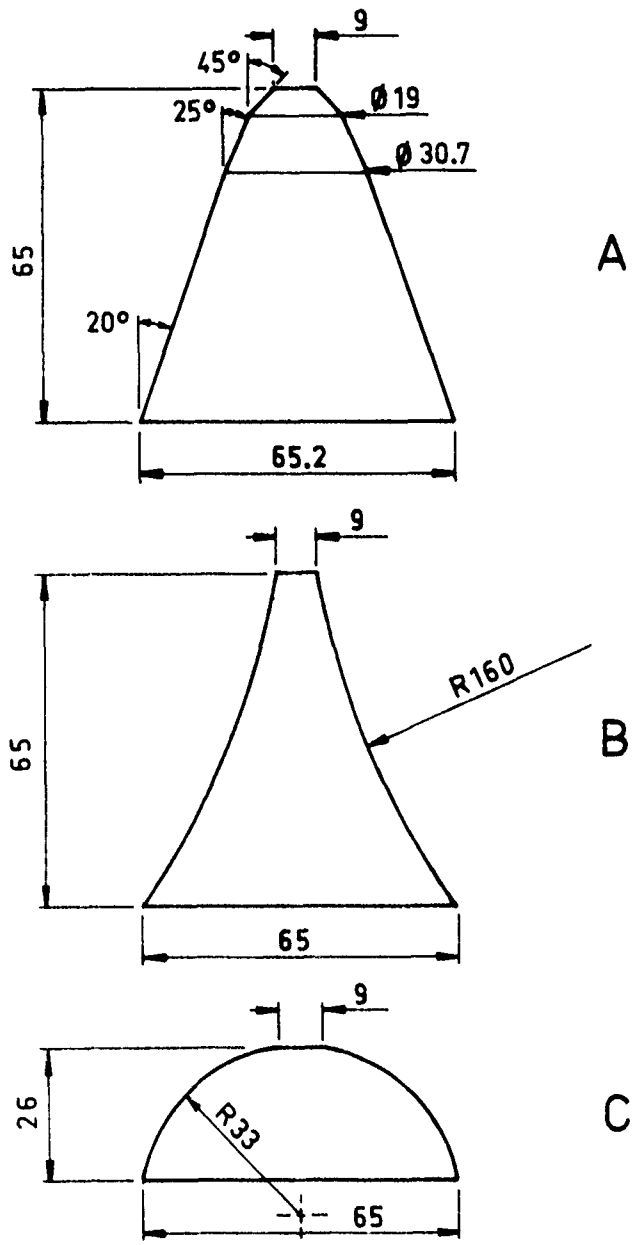

Figure 1(b). Missile nose shapes used with Mk I wind direction sensor

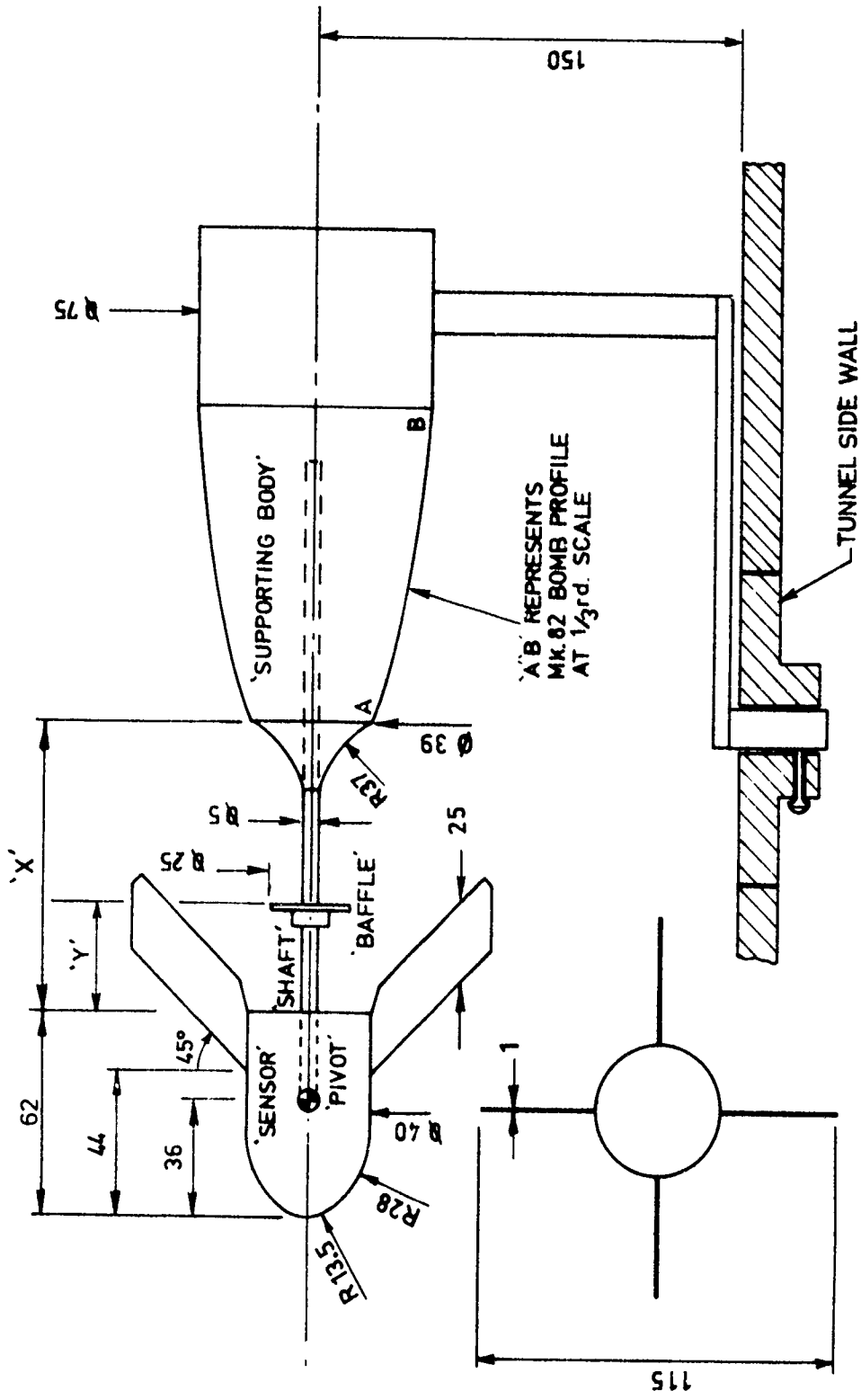

Figure 2. Mk II wind direction sensor

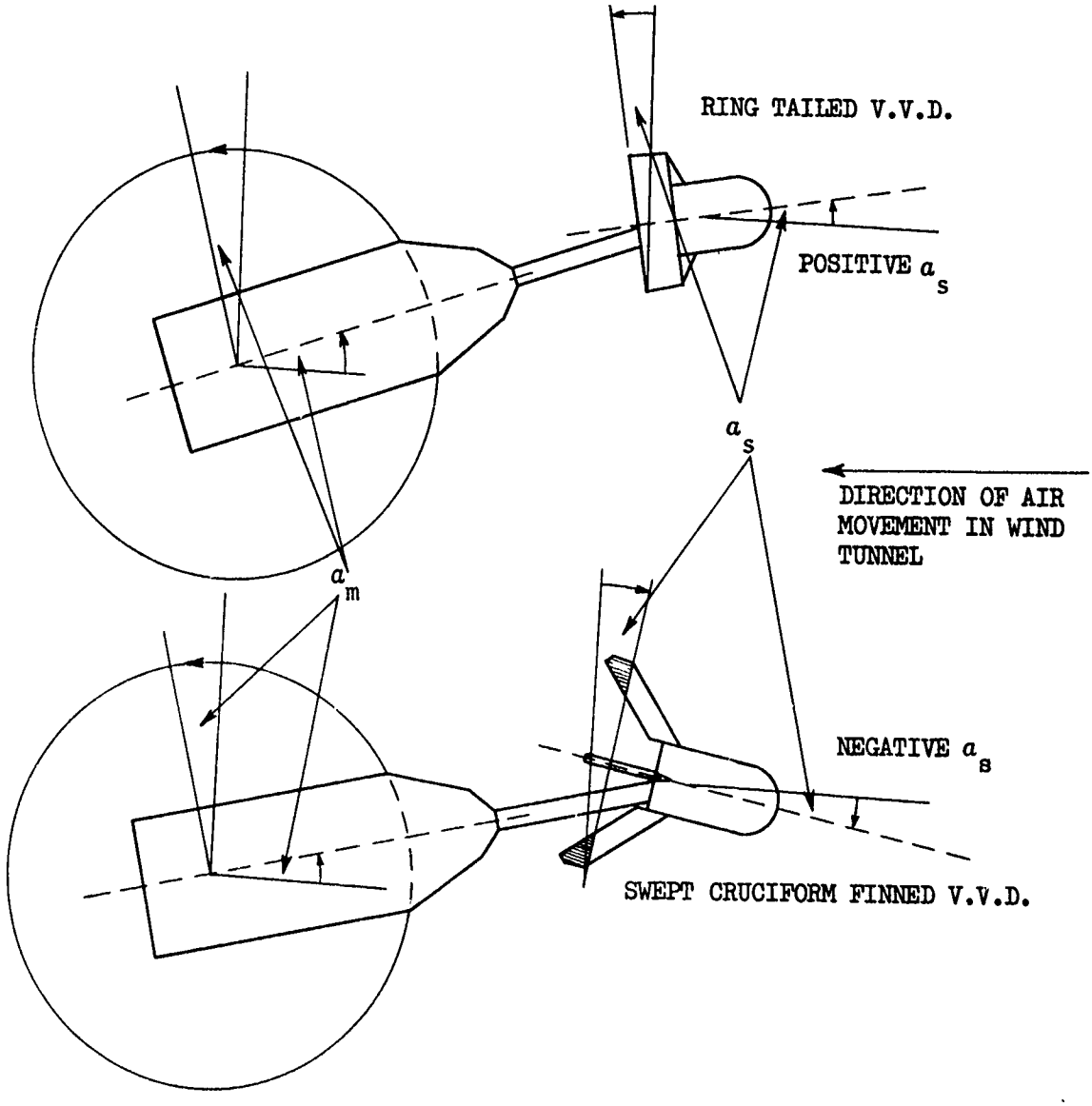

Figure 3. Measurement of a_m, a_s

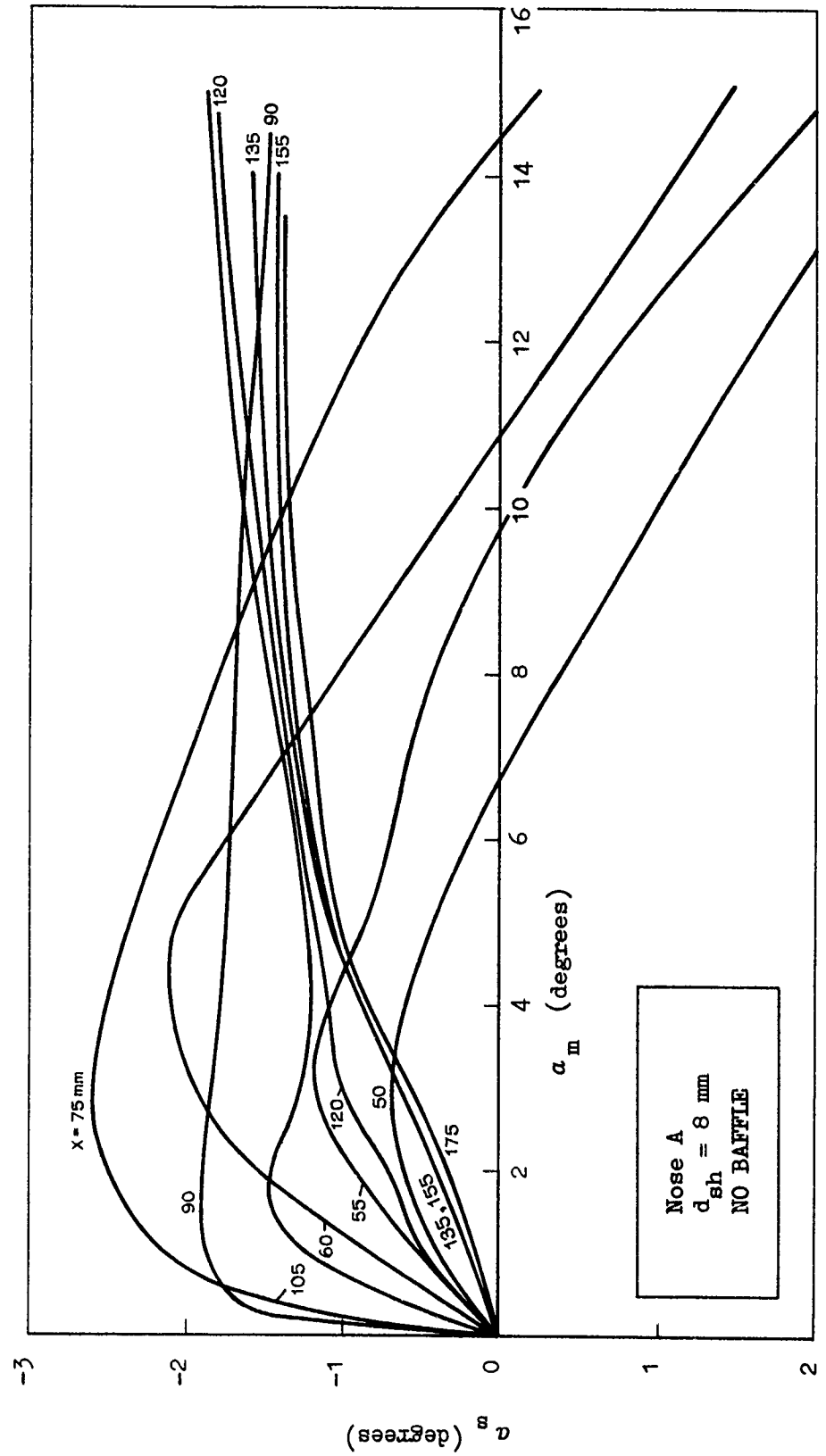

Figure 4. Mk I sensor alignment with noses A, B and C

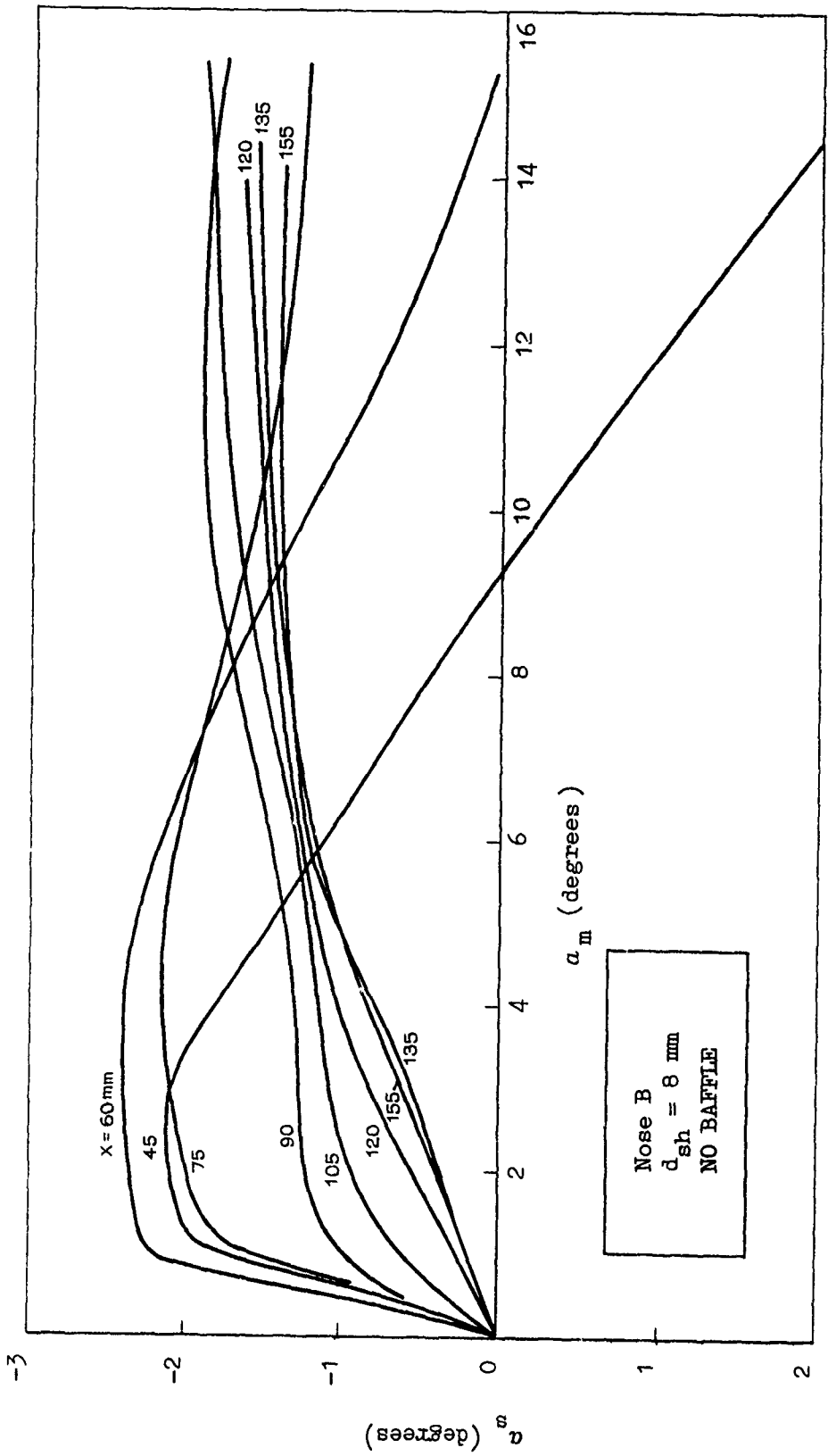

Figure 4 (cont). Mk I sensor alignment with noses A, B and C

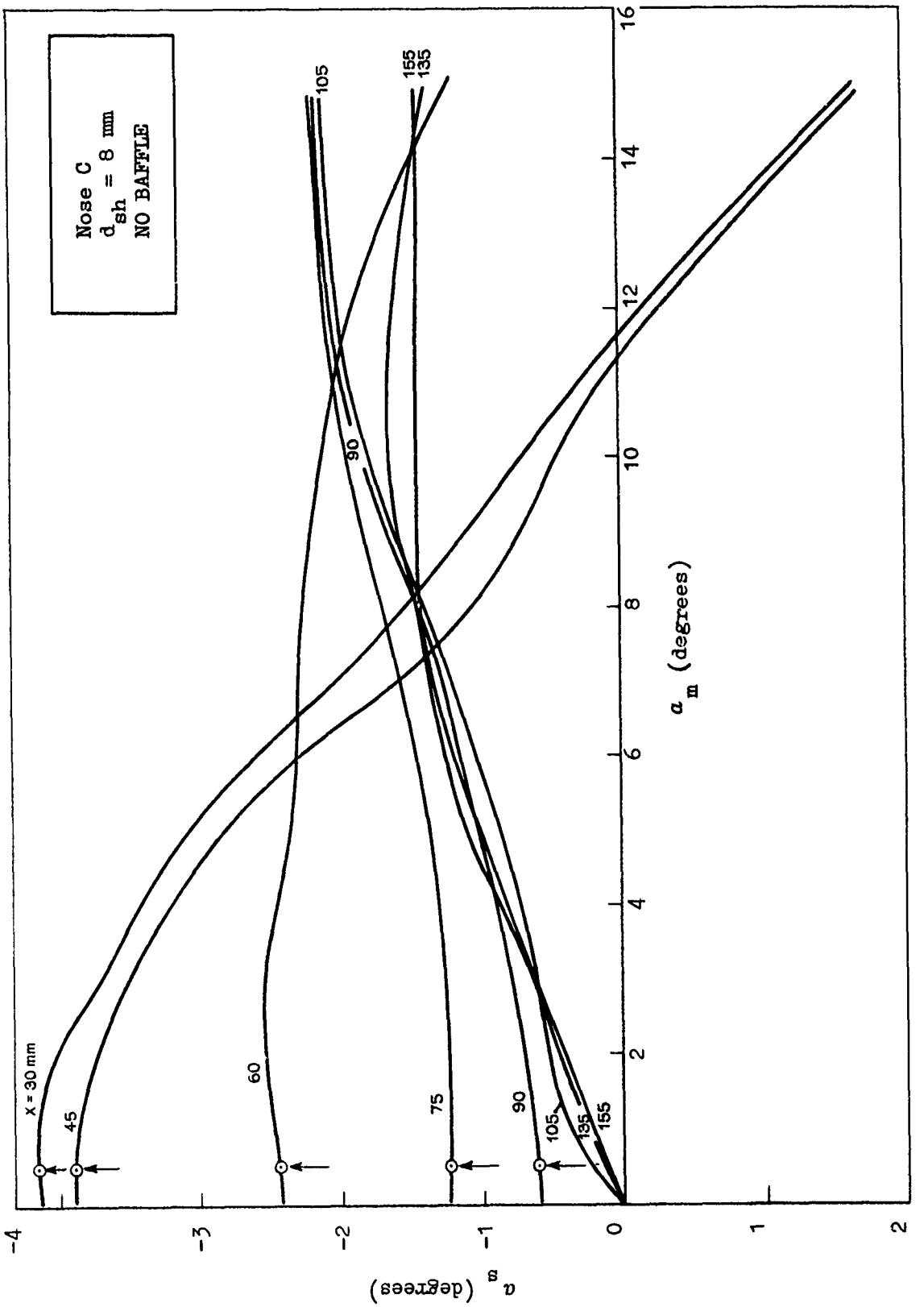

Figure 4 (cont). Mk I sensor alignment with noses A, B and C

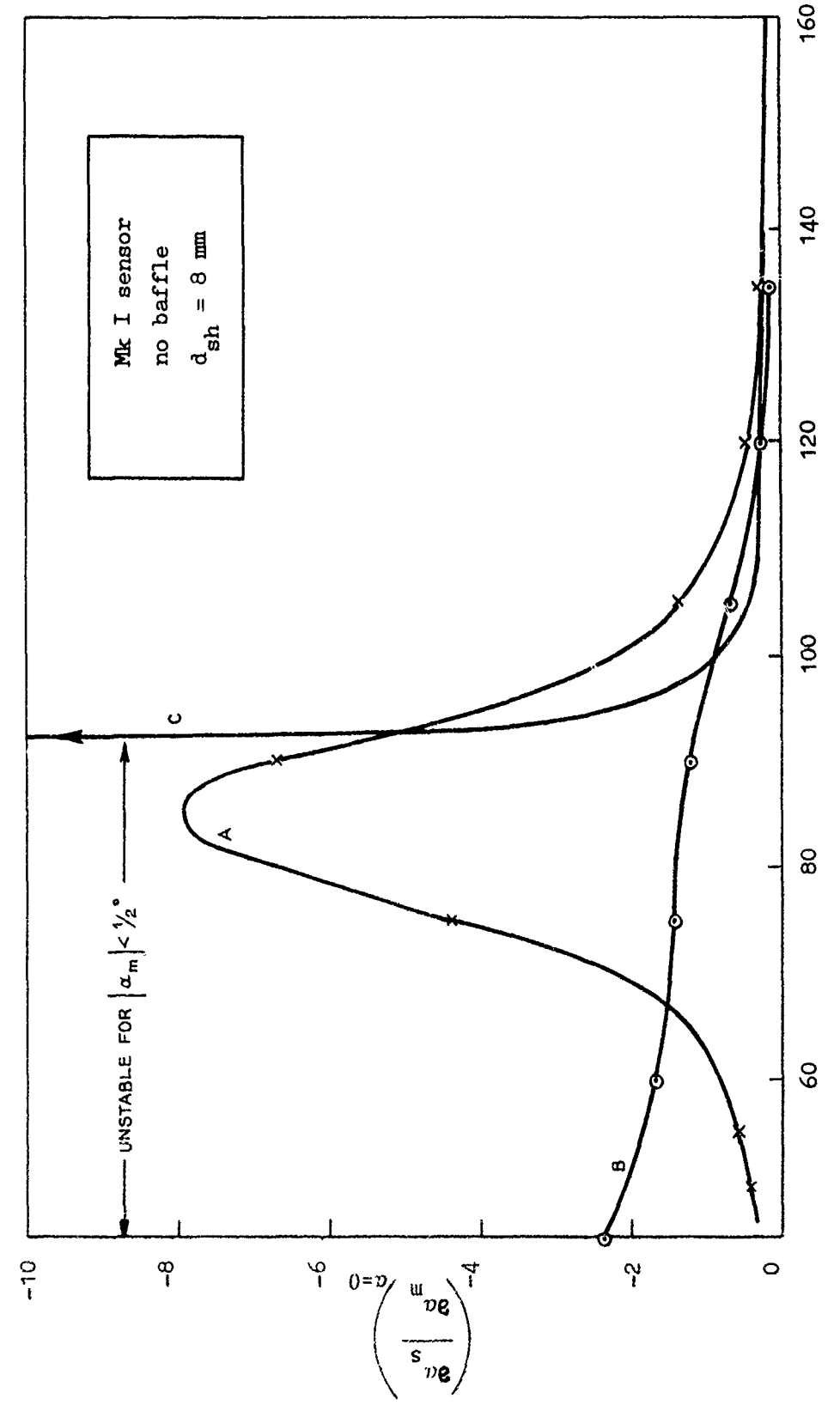

Figure 5. $\left(\partial \alpha_s / \partial \alpha_m\right)_{\alpha=0}$ versus X for various missile nose shapes

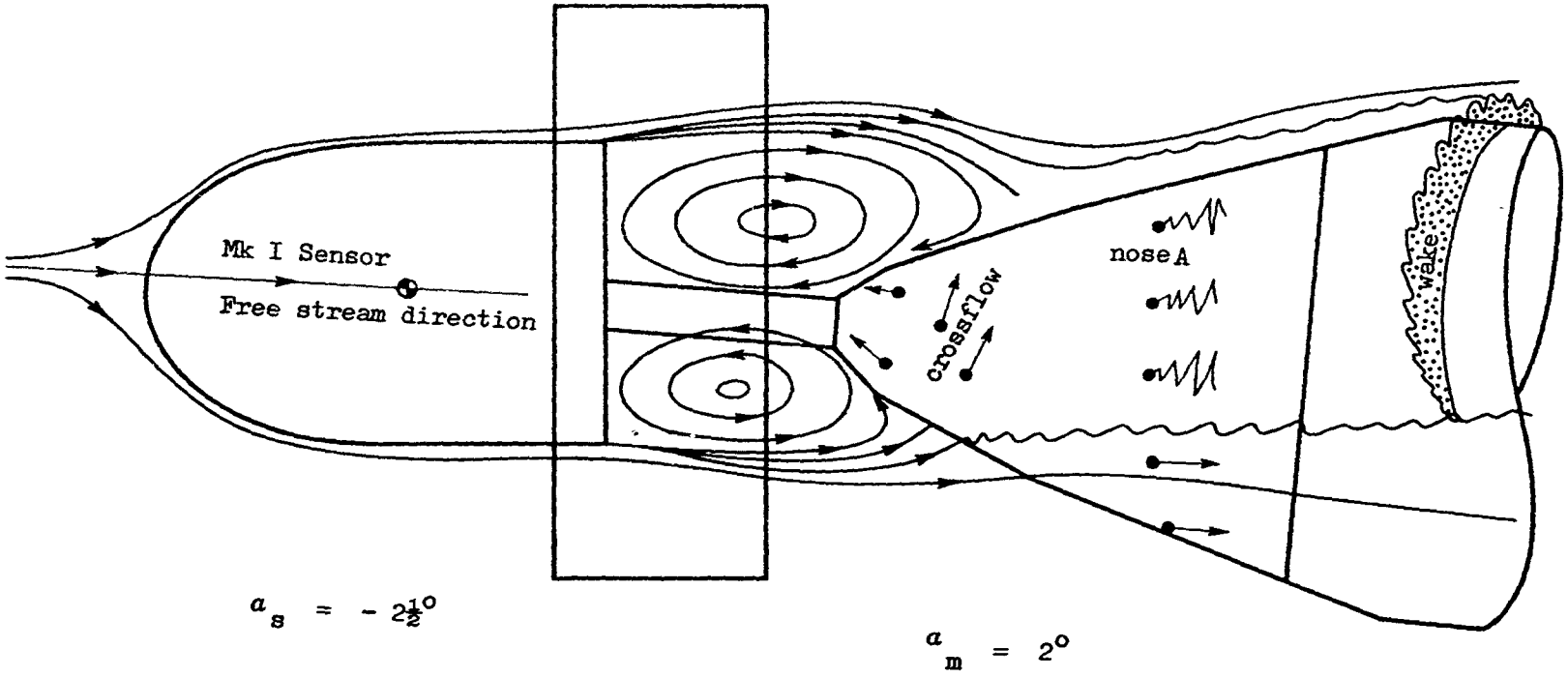

Figure 6. Flowfield in angle-of-attack plane

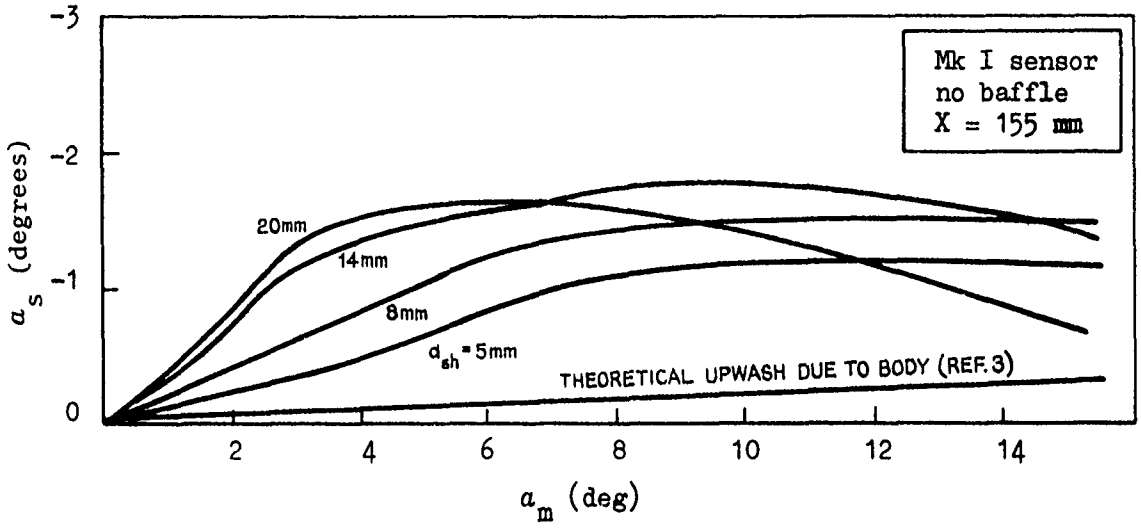

(a) a_s versus a_m for various shaft diameters

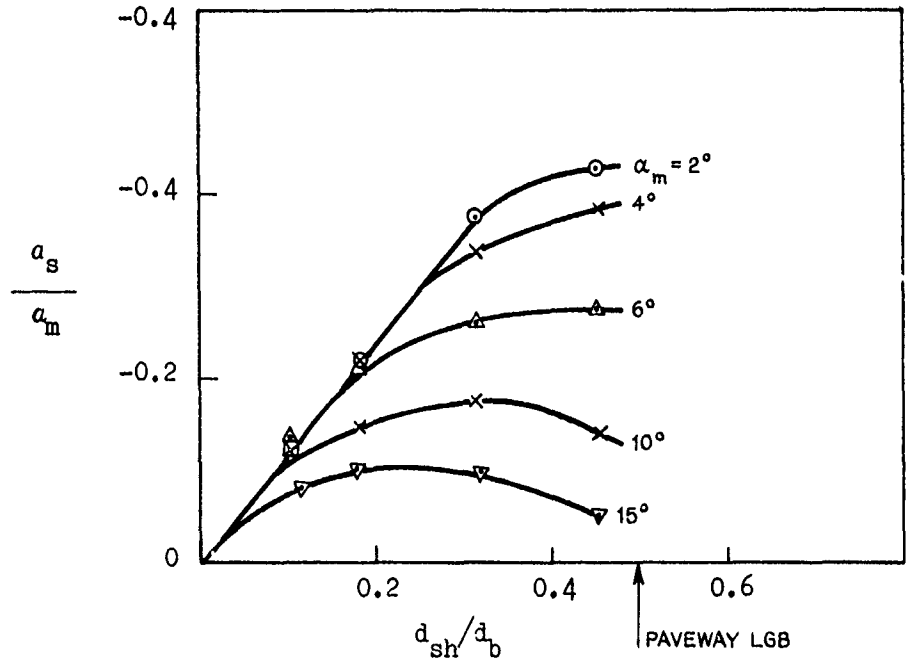

(b) a_s/a_m versus d_{sh}/d_b for various a_m

Figure 7. Mk I sensor alignment for long shafts of various diameters

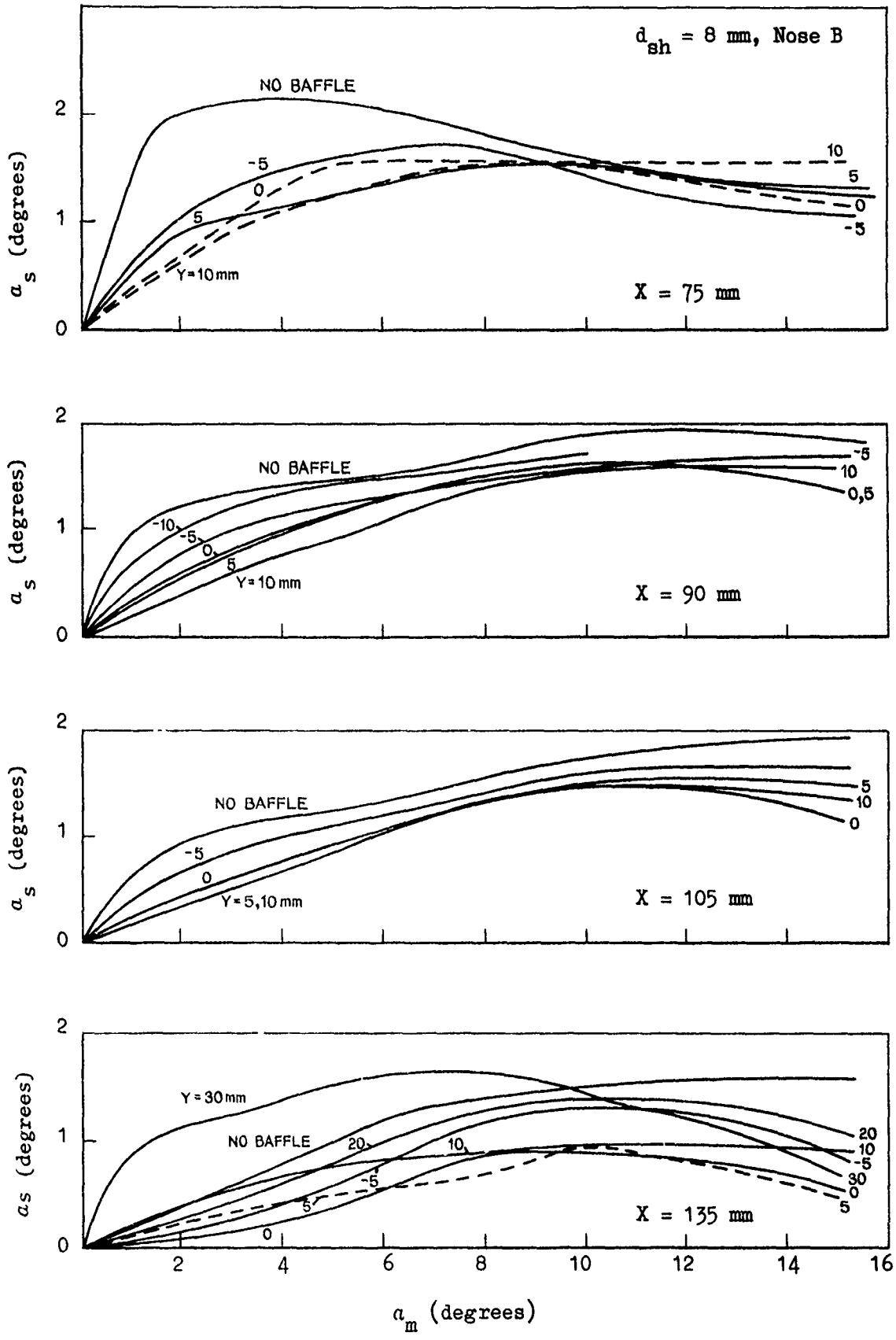

Figure 8. Effect of baffle position on Mk I sensor alignment nose B

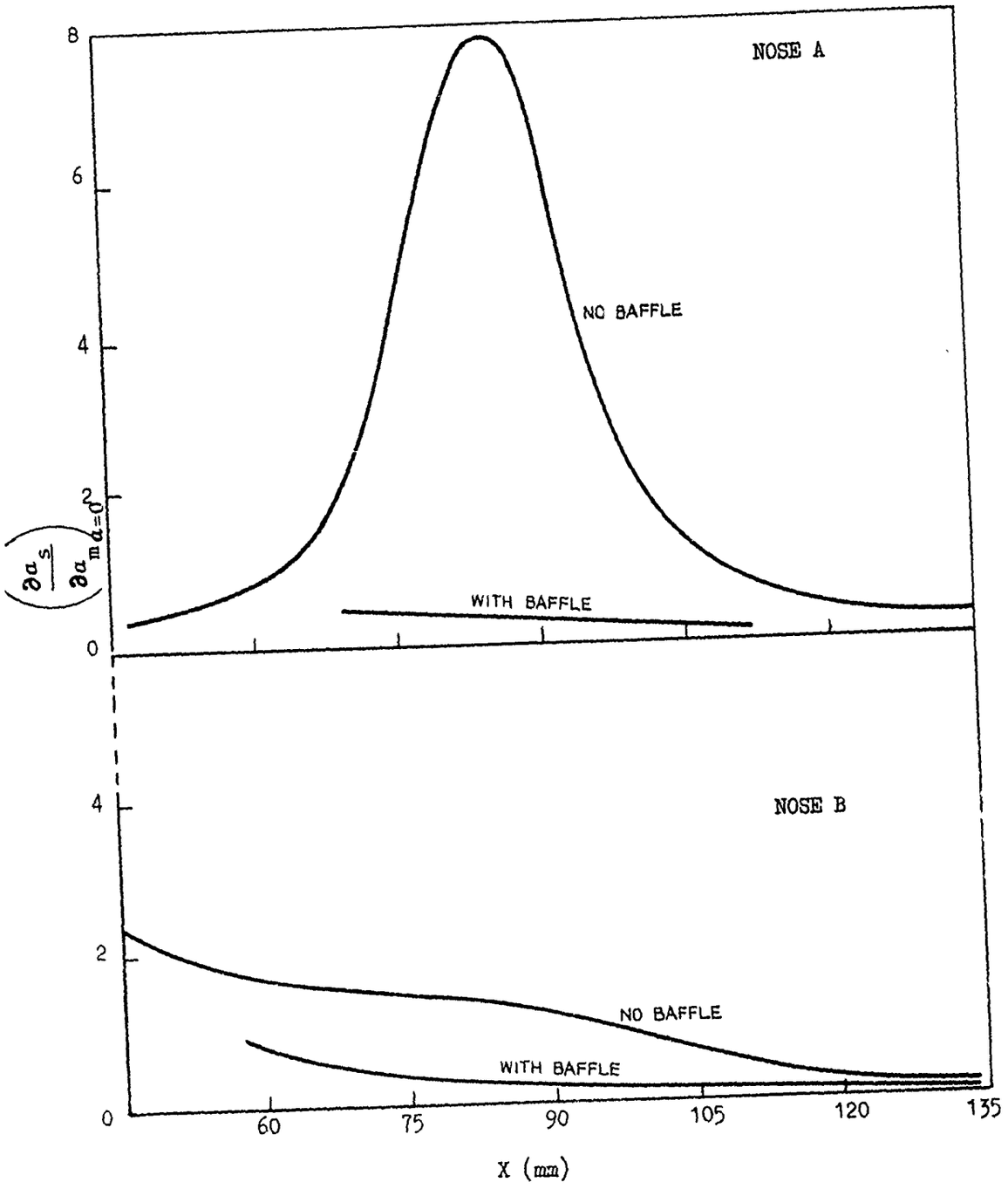

Figure 9. Maximum reduction in misalignment sensitivity produced by baffle

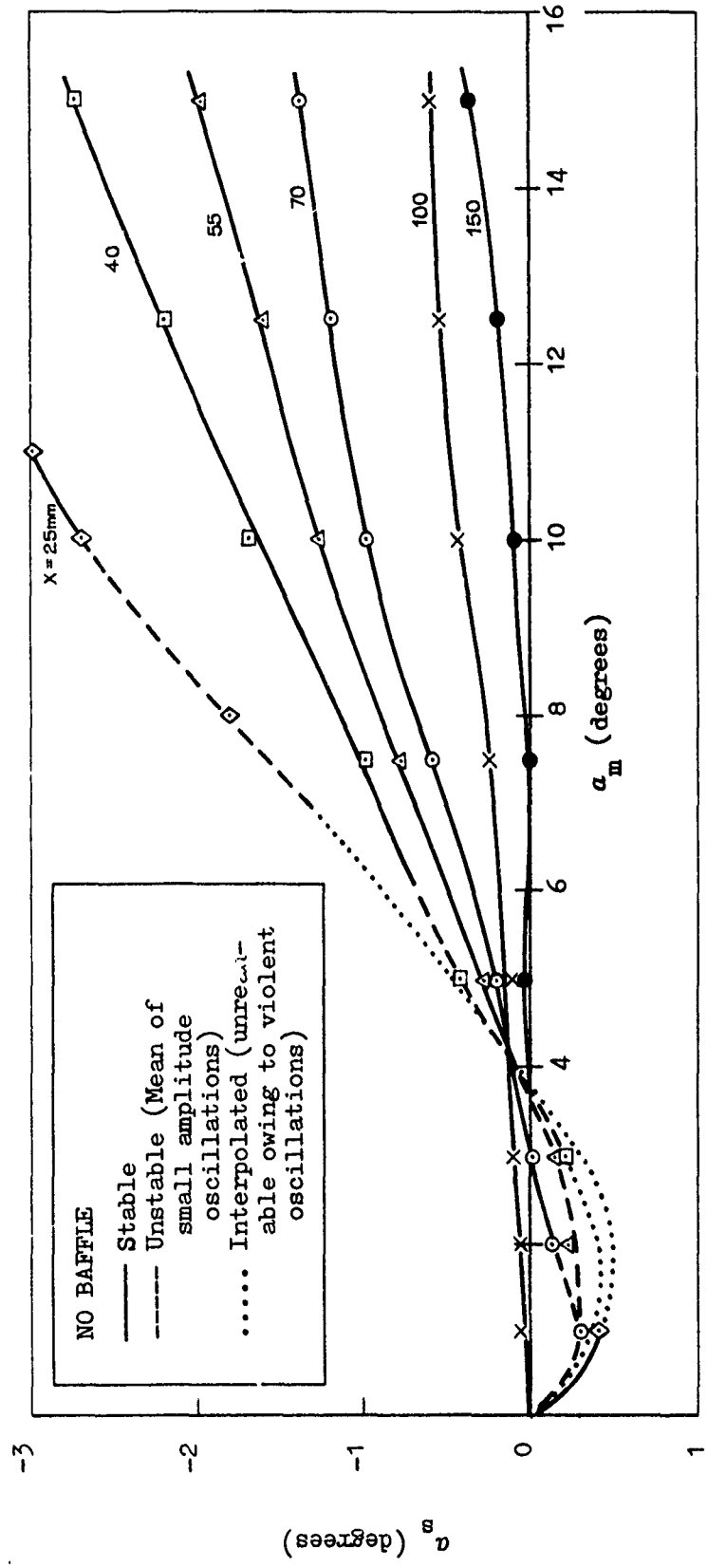

Figure 10. Mk II sensor alignment

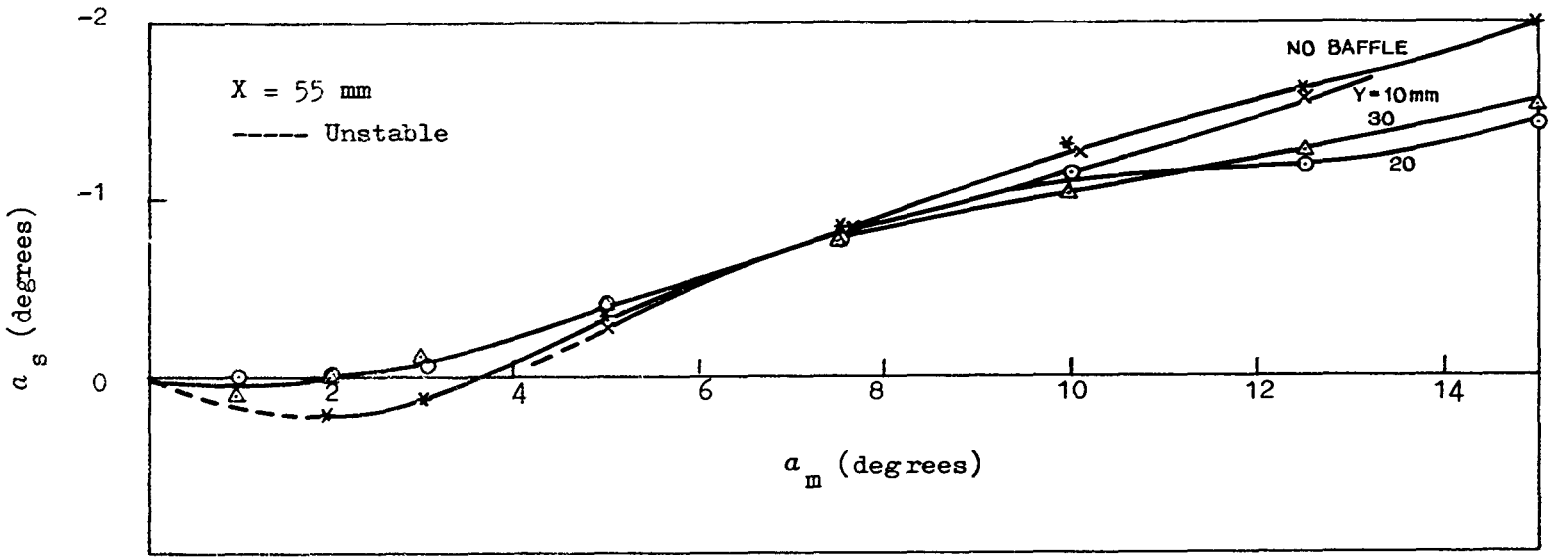

(a) Effect of baffle

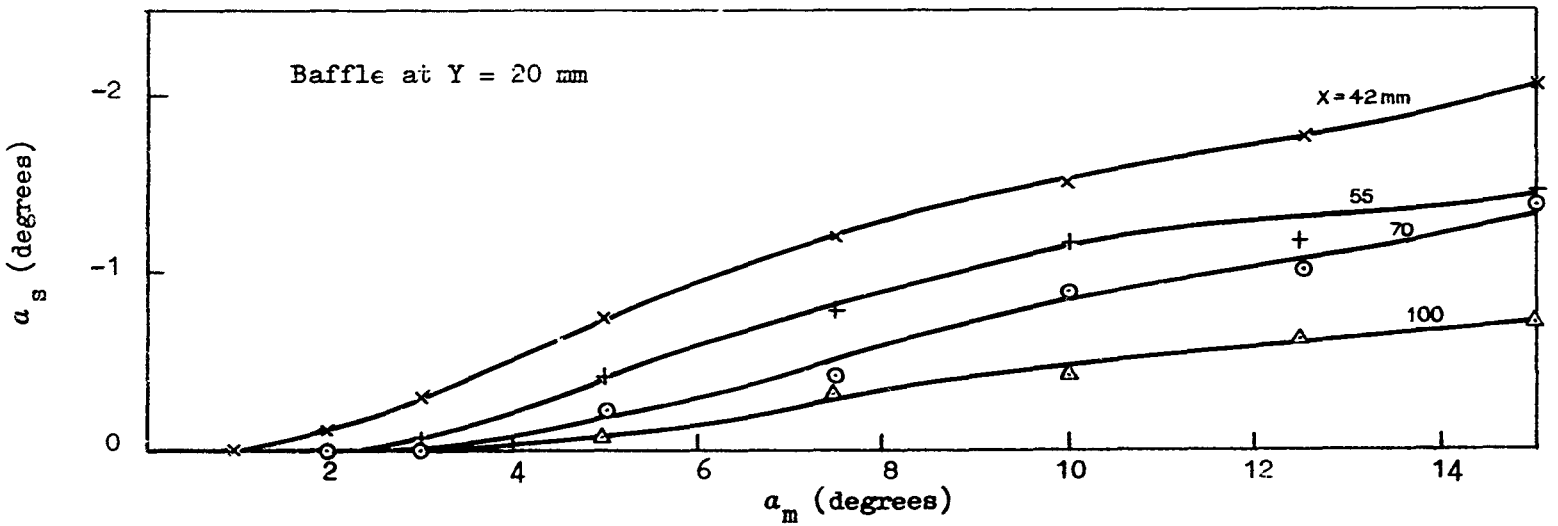

(b) Effect of separation distance, X

Figure 11. Mk II sensor plus baffle

DISTRIBUTION

	Copy No.
EXTERNAL	
In United Kingdom	
Defence Scientific and Technical Representative, London	1
British Library Lending Division, Boston Spa Yorkshire, UK	2
In United States of America	
Counsellor, Defence Science, Washington	3
National Technical Information Service, Springfield Va USA	4
NASA Scientific and Technical Information Office, Washington DC USA	5
Engineering Societies Library, New York NY USA	6
In Australia	
Chief Defence Scientist	7
Deputy Chief Defence Scientist	8
Superintendent, Science and Technology Programmes	9
Army Scientific Adviser	10
Navy Scientific Adviser	11
Air Force Scientific Adviser	12
Superintendent, Analytical Studies	13
Director, Material Assessments (Science)	14
Director, Programme Management (Science)	15
Controller, Projects and Analytical Studies	16
Defence Information Services Branch (for microfilming)	17
United Kingdom, Ministry of Defence, Defence Research Information Centre (DRIC)	18
United States, Department of Defense, Defense Documentation Center	19 - 30
Canada, Department of National Defence, Defence Science Information Service	31
New Zealand, Ministry of Defence	32
Australian National Library	33